Incorporation of [Cp*Rh] and [Cp*Ir] Species into Heterobimetallic Complexes via Protonolysis Reactivity and Dioximato Chelation

Amit Kumar,[#] Daniel S. King,[#,†] Victor W. Day,[#] and James D. Blakemore[#*]

[#]Department of Chemistry, University of Kansas, 1567 Irving Hill Road, Lawrence, Kansas 66045, United States

Supporting Information Placeholder

ABSTRACT: Synthesis of multimetallic compounds can enable placement of two or more metals in close proximity, but efforts in this area are often hindered by reagent incompatibilities and lack of selectivity. Here, we show that organometallic half-sandwich [Cp*M] (M = Rh, Ir) fragments (where Cp* is η^5-pentamethylcyclopentadienyl) can be cleanly installed into metallomacrocyclic structures based on the workhorse diimine-monooxime-monooximato ligand system. Six new heterobimetallic compounds have been prepared to explore this synthetic chemistry, which relies on *in situ* protonolysis reactivity with precursor Ni(II) or Co(III) monometallic complexes in the presence of suitable [Cp*M] species. Solid-state X-ray diffraction studies confirm installation of the [Cp*M] fragments into the metallomacrocyles via effective chelation of the Rh(III) and Ir(III) centers by the nascent dioximato site. Contrasting with square-planar Ni(II) centers, the Co(III) centers prefer octahedral geometry in the heterobimetallic compounds, promoting bridging ligation of acetate across the two metals. Spectroscopic and electrochemical studies reveal subtle influences of the metals on each other's properties, consistent with the moderate M'•••M distances of ca. 3.6–3.7 Å in the modular compounds. The [Co,Rh] complex was found to catalyze hydrogenation of *p*-trifluoromethylbenzaldehyde to *p*-trifluoromethylbenzyl alcohol more cleanly than a 1:1 mixture of the individual monometallic precursor complexes, suggesting that this family of heterobimetallic complexes could be useful in future studies of multimetallic chemistry, especially in light of the starring role of other [Cp*M] complexes in diverse catalytic systems.

1. INTRODUCTION

Bringing two different metal centers into close proximity attracts considerable interest across a number of research areas. This is in part due to the unique properties and cooperativity that can be engendered in such compounds in comparison to their monometallic analogues.[1,2] Bimetallic complexes incorporating redox-active centers are especially notable for their redox flexibility and, often, improved substrate-binding capabilities. Indeed, nature takes advantage of multimetallic systems in many metalloenzymes capable of small-molecule activation. The oxygen-evolving complex (OEC) of Photosystem II utilizes four Mn centers and a conserved redox-inactive Ca^{2+} ion to catalyze the oxidation of water to oxygen.[3] Other multimetallic active sites perform reduction reactions such as conversion of O_2 by [Cu,Fe] cytochrome *c* oxidase,[4] fixation of N_2 by Fe- and Mo-containing nitrogenase,[5] and reduction of protons to dihydrogen by NiFe hydrogenase.[6] Inspired by these systems, many researchers have endeavored to design artificial metal complexes that engender synergistic involvement of multiple metals.[7] One especially vigorous area of investigation centers on use of secondary redox-inactive metals to tune the chemical properties of primary redox-active metal centers,[8,9,10] an approach of particular interest to us considering its versatility.[11,12,13] However, a unifying theme of all this work is the bringing together of two metals selectively, enabling studies of their individual roles in observed reactivity.

Tetraazamacrocyclic complexes containing the earth-abundant metals nickel and cobalt are perhaps best known as catalysts for electrochemical hydrogen generation.[14,15] A subset of these complexes can be derivatized by placement of a cationic [BF_2] bridging moiety in place of a bridging proton (H^+).[16,17] Such reactivity is conceptually related to the early work of Busch and co-workers regarding glyoxime-type ligands and their macrocyclic metal complexes.[18] However, metal complexes supported by proton-bridged macrocyclic diimine-monooxime-monooximato-type ligand frameworks have also been attractive as synthons for construction of bimetallic complexes. Chaudhuri, Wieghardt, and co-workers were perhaps the first to realize potential in this space, and showed that a variety of first-row transition metals (Cr, Mn, Fe, Co, Ni, Cu) could be installed divergently in the dioximato site (see Chart 1).[19] Peter & co-workers leveraged the binucleating nature of these ligands to install Mg and Zn in close proximity to Co and Ni metal centers.[20] And, more recently, Cossairt and co-workers extended this approach further to incorporation of 4*d* metals, isolating [Co,Ru] and [Co,Cd] complexes.[21] A general feature uniting all this work is the net removal of a proton from the dioximato site and installation of a cationic metal fragment in its place.

Chart 1. Heterobimetallic complexes based upon diimine-monooxime-monooximato ligands.

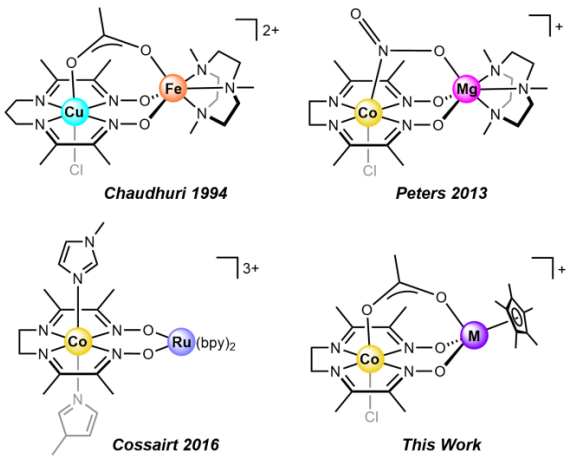

Half-sandwich Group 9 metal complexes supported by Cp* ligands (where Cp* is η^5-pentamethylcyclopentadienyl) represent a useful and synthetically versatile class of organometallic species.[22] Structures containing [Cp*M] fragments tend to be quite stable, due to the steric bulk and strong donor properties of Cp*,[23] but can also serve as catalysts for a variety of transformations.[24] In our own work, we have relied on the synthetic versatility of [Cp*Rh] complexes in particular, for preparation of new metal complexes useful for studies of proton management during catalysis.[25] In the context of this work, we examined the literature and were surprised to find no prior synthetic work aimed at incorporating organometallic fragments like the [Cp*Rh] or [Cp*Ir] cores into metal complexes bearing dioximato sites. However, considering the successful prior work on bimetallic coordination compounds supported by diimine-dioximato ligands, we anticipated that the modularity of this chemistry might enable preparation of new heterobimetallic compounds containing organometallic [Cp*M] sites.

Here, we report two general procedures for synthesis of heterobimetallic complexes based upon diimine-dioximato ligands that incorporate half-sandwich [Cp*M] fragments (where M is Rh or Ir). The first procedure relies on $Cp^*M(OAc)_2$ precursor complexes, denoted as **M-OAc** hereafter, which contain acetate ligands that can undergo protonolysis by the bridging protons present in monometallic Ni(II) and Co(III) diimine-monoxime-monooximato precursor complexes. The second procedure utilizes more common $[Cp^*MCl_2]_2$ precursors in concert with exogeneous NaOAc, and is a useful route for generation of chloride-containing heterobimetallic complexes of Ni(II). Using these protonolysis-driven procedures, we have prepared and fully characterized six new heterobimetallic complexes containing [Cp*Rh] or [Cp*Ir] fragments contained within diimine-dioximato chelating frameworks. In these systems, the tetraazamacrocylic core functions as a heteroditopic ligand, hosting either Ni(II) or Co(III) in its central tetradentate site and either Rh(III) or Ir(III) in its peripheral bidentate site. These complexes are the first examples of structurally characterized oxime-bridged heterobimetallics containing [Cp*Rh] and [Cp*Ir] moieties paired with 3*d* metals.[26] Solid-state X-ray diffraction studies along with spectroscopic and electrochemical investigations have been used to study the properties of the new heterobimetallic complexes. On the basis of the findings, we conclude that these complexes could be useful for studies of heterobimetallic chemistry involving organometallic species.

2. RESULTS

2.1 Synthesis and Characterization

In order to prepare the target heterobimetallic complexes, we first synthesized precursor monometallic complexes supported by tetradentate diimine-dioxime-type ligands. We turned to the known ligands commonly abbreviated as $(DOH)_2$pn and $(DOH)_2$en for preparation of Ni(II) and Co(III) complexes, respectively.[27] $(DOH)_2$pn represents the diimine-dioxime-type ligand bridged by 1,3-propanediamine, while $(DOH)_2$en is bridged by ethylenediamine (see Scheme 1). Both ligands were prepared from diacetylmonoxime using literature procedures,[28] and no unusual features were encountered in either case. We selected these two different ligands for this work, because, in our hands, the $(DOH)_2$pn ligand could be used to generate clean nickel complexes, but was not suitable for generation of isolable cobalt complexes.

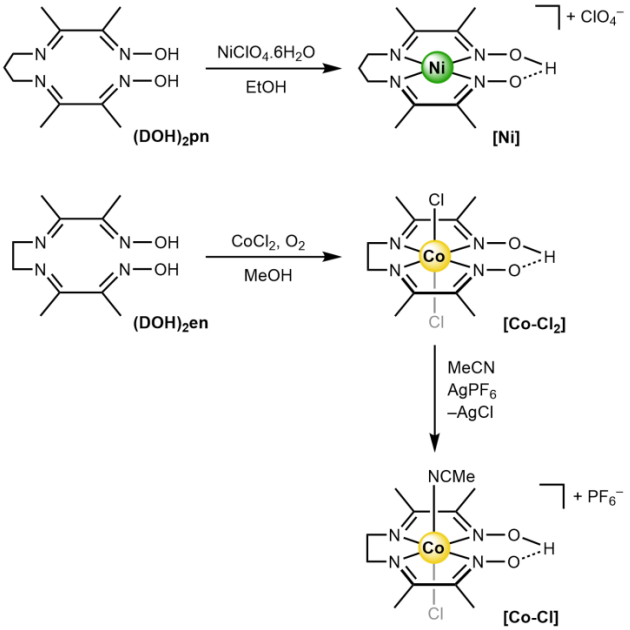

Scheme 1. Synthesis of nickel(II) and cobalt(III) monometallic complexes.

We synthesized the monometallic Ni(II) and Co(III) precursor complexes using literature procedures involving reaction of nickel perchlorate hexahydrate and cobalt dichloride with 1 equivalent of $(DOH)_2$pn or $(DOH)_2$en, respectively.[27,28] The desired monometallic complexes, $[Ni(DO)(DOH)pn]ClO_4$ and $CoCl_2(DO)(DOH)$en, referred to hereafter as **Ni** and **Co-Cl$_2$**, respectively (see Scheme 1), contain the key proton-bridged macrocyclic structures that enable preparation of heterobimetallic species. **Ni** was first prepared by Uhlig and Friedrich while **Co-Cl$_2$** was first prepared by Marzilli.[27,29] In order to assemble the desired heterobimetallic complexes containing cobalt, however, we further prepared a new form of the complex, **Co-Cl**, by salt metathesis of **Co-Cl$_2$** with $AgPF_6$, to generate the desired monochloride species (*vide infra*). The **Co-Cl** complex could be isolated and was characterized by ^{1}H NMR (see Experimental Section), but was used here only for preparation of the target heterobimetallics. Based on ^{1}H NMR, **Co-Cl** is associated with a single bound acetonitrile solvent molecule, confirming the effectiveness of the desired salt metathesis reactivity (see SI, Figure S10).

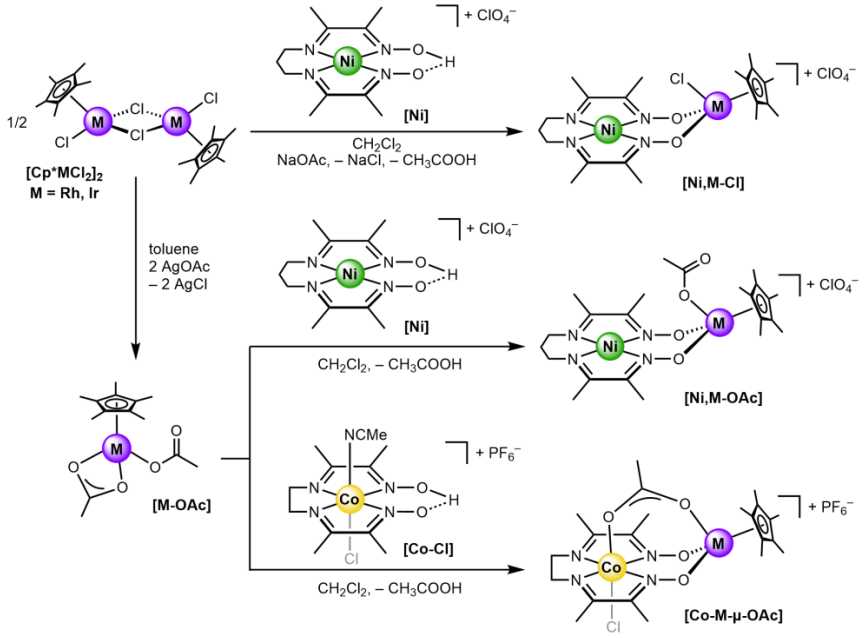

Scheme 2. Synthesis of heterobimetallic complexes of nickel(II) and cobalt(III) with rhodium(III) and iridium(III) secondary metals.

With both **Ni** and **Co-Cl** in hand, heterobimetallic complexes pairing the Ni(II) and Co(III) metal centers with [Cp*Rh] or [Cp*Ir] centers bearing acetate ions could be prepared by stirring with 1 equiv. of the appropriate $Cp^*M(OAc)_2$ precursors (abbreviated as **M-OAc**) in dichloromethane, respectively. The desired heterobimetallic complexes were obtained following workup in good to excellent yields (>85%) in all cases (see Experimental Section). In the reactions, the distinct smell of acetic acid could be identified in the environment of the reaction vial, confirming the desired protonolysis reactivity that affords the desired **Ni,Rh-OAc**, **Ni,Ir-OAc**, **Co,Rh-μ-OAc**, and **Co,Ir-μ-OAc** (see Scheme 2). Additionally, $[Cp^*RhCl_2]_2$ and $[Cp^*IrCl_2]_2$ could be used directly for generation of chloride-bound analogues of the nickel complexes.[30] This alternative procedure provided heterobimetallic complexes of the form **Ni,Rh-Cl** and **Ni,Ir-Cl** (see Scheme 2). Yields of these reactions were also good to excellent. Considering the clean protonolysis reactivity that we observed, we note that Peters[20] and Cossairt[21] utilized nitrogen-containing organic bases for installation of divalent metal ions in dioximato sites (see Chart 1). Our synthetic procedure is distinctive from these cases, since our byproducts of protonolysis and salt metathesis (acetic acid and sodium chloride, respectively) can be conveniently separated by filtration and removal of all volatiles *in vacuo*. Appealingly, all of the six new heterobimetallic complexes described here are diamagnetic; ^{1}H NMR resonances corresponding to the methyl groups on the diimine-dioximato metallomacrocycle appear as two singlets in CD_3CN, consistent with a C_s-symmetric appearance of the bimetallic complexes in solution (see SI for all NMR spectra). A single, intense resonance corresponding to the five equivalent methyl groups of the η^5-Cp* ligand was also observed, confirming free rotation in solution. ^{1}H, ^{31}P, and ^{19}F NMR studies as well as elemental analysis of all the isolated materials were successfully obtained, confirming generation and clean isolation of the desired compounds (see SI and Experimental section for details).

2.2 X-ray Diffraction Studies

Single crystals suitable for X-ray diffraction (XRD) analysis were obtained for all of the heterobimetallic complexes reported here. Crystals of five of the six compounds were grown by vapor diffusion of diethyl ether into concentrated acetonitrile solutions of the desired complexes, while one exception was **Ni,Ir-Cl** which required diffusion of diethyl ether into a concentrated methanol solution of the complex. XRD analysis revealed the geometries around the Ni(II) centers to be square-planar in all cases, and around the Co(III) centers to be octahedral in all cases. Additionally, the geometries around the Rh and Ir centers were found to be *pseudo*-octahedral in all cases.

Solid-state structures of the Ni(II) complexes **Ni,M-Cl** and **Ni,M-OAc** (M = Rh or Ir) (Figure 1 and Figure 2) reveal a preference for highly planar environments around the nickel centers. The planarity of the tetradentate sites containing nickel could be quantified in our diffraction data through the ω_{N4} parameter, which was defined here as the root-mean-square deviation of the four nitrogen donor atoms from the mean plane defined by the positions of those atoms. Inspection of the data (see Table 1) reveals that the value of the ω_{N4} parameter is very small for the monometallic precursor **Ni** at 0.006, and increases only slightly for each of the heterobimetallic complexes. On the other hand, the Ni(II) metal centers situated in the tetradentate sites are modestly displaced from the rather planar macrocyclic structures, as quantified with the $\psi_{M'}$ values given in Table 1. In particular, the Ni(II) centers are displaced by ≥ 0.6 Å in all the relevant heterobimetallic complexes, implicating weak axial interactions and/or ligand distortions that affect the metal center. The secondary metals M (Rh or Ir) are not located in the plane containing the macrocyclic N and O atoms in any case; this displacement was quantified by the ϕ angle, representing the angle between the plane defined by N1, N2, N3, N4, O1, O2 and the plane defined by O1, O2, and Rh/Ir. The ϕ angle increases slightly for **Ni,Ir-OAc** in comparison to the other derivatives, perhaps consistent with the larger size of Ir and steric demand of acetate versus chloride. Overall, however, all the nickel complexes closely resemble each other on the basis of all the structural metrics (see Table 1).

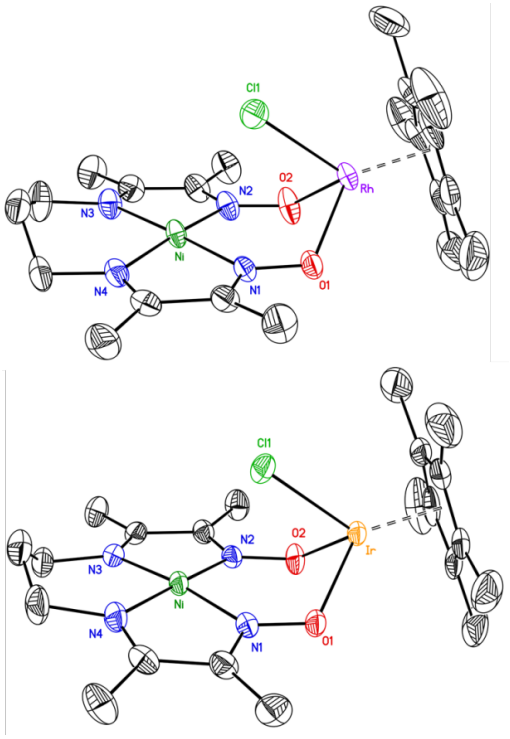

Figure 1. Solid-state structure from XRD of **Ni,Rh-Cl** (upper structure) and **Ni,Ir-Cl** (lower structure). All H-atoms, the outer-sphere perchlorate counteranion and co-crystallized CH_3CN solvent molecule are omitted for clarity. Displacement ellipsoids are shown at the 50% probability level.

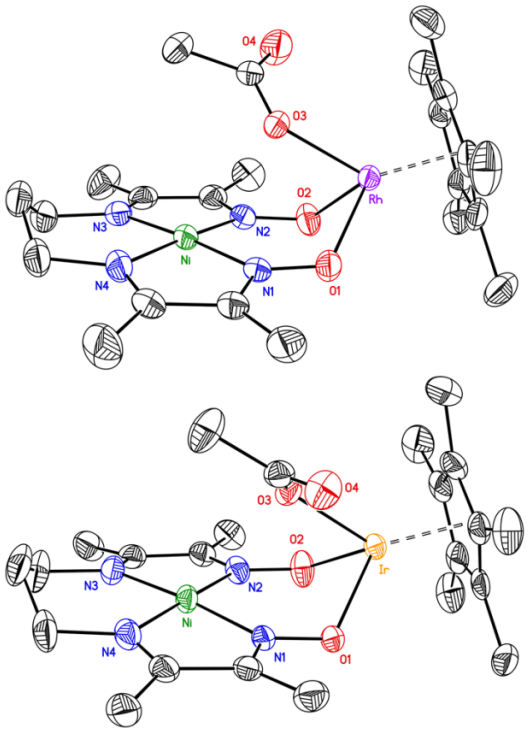

Figure 2. Solid-state structure from XRD of **Ni,Rh-OAc** (upper structure) and **Ni,Ir-OAc** (lower structure). All H-atoms, the outer-sphere perchlorate counteranion and co-crystallized CH_3CN solvent molecule are omitted for clarity. Displacement ellipsoids are shown at the 50% probability level.

Table 1. Comparison of structural parameters from X-ray diffraction studies

Compound	Ni[a]	Ni,Rh-Cl	Ni,Ir-Cl	Ni,Rh-OAc	Ni,Ir-OAc	Co-Cl_2[b]	Co,Rh-μ-OAc[c]	Co,Ir-μ-OAc[c]
M′•••M (Å)[d]	-	3.649(1)	3.677(1)	3.664(1)	3.725(1)	-	3.606(1)	3.643(1)
M–Cp*$_{cent}$ (Å)[e]	-	1.746	1.757	1.751	1.749	-	1.742	1.745
M–O_{avg} (Å)[f]	-	2.091(4)	2.099(4)	2.100(3)	2.102(4)	-	2.104(3)	2.100(4)
N–O_{avg} (Å)	1.336(3)	1.323(6)	1.336(6)	1.318(4)	1.325(6)	1.333(1)	1.319(4)	1.320(6)
M′–N_{avg} (Å)	1.882(3)	1.901(6)	1.898(6)	1.904(6)	1.902(8)	1.863(1)	1.880(5)	1.878(6)
O1•••O2 (Å)	2.420(2)	2.785(4)	2.771(4)	2.781(3)	2.770(4)	2.697(1)	3.062(3)	3.039(4)
∠ NOM_{avg} (°)	-	118.0(3)	118.9(3)	118.5(2)	120.1(3)	-	117.7(2)	119.2(3)
∠ XMC_{cent} (°) (X = Cl or O)	-	126.3	126.6	132.8	133.2	-	121.3	122.7
ϕ (°)[g]	-	124.9	125.6	125.1	128.3	-	135.2	137.3
ω_{N4} [h]	0.006	0.038	0.029	0.004	0.020	0.030	0.029	0.024
$\psi_{M'}$[i] **(Å)**	0.014	0.064	0.086	0.066	0.060	0.085	0.115	0.114

(a) Structural data taken from references 14 and 31 (CCDC 738487). (b) Structural data taken from references 28 and 32 (CCDC 646793). (c) **Co,Rh-μ-OAc** and **Co,Ir-μ-OAc** crystallize with isomorphous structures. (d) Here **M′** denotes Ni or Co and **M** denotes Rh or Ir. (e) Distance between centroid of the pentamethylcyclopentadienyl (Cp*) ring and Rh/Ir metal. (f) Errors on the average bond lengths and bond angles were derived by propagation of error from the individual values and estimated standard deviations (e.s.d.'s). (g) The angle between the plane defined by N1, N2, N3, N4, O1, O2 and the plane defined by Rh/Ir, O1, O2. (h) Defined as the root mean square deviation (r.m.s.d.) of the following atoms from the mean plane of their positions: N1, N2, N3, and N4. (i) Defined as the distance between the Ni/Co and the centroid of the plane defined by N1, N2, N3, and N4. All atom labels are consistent with those given in the crystallographic data (see Supporting Information).

The first coordination spheres of the Rh and Ir centers contain the η^5-Cp* ligand, the κ^2-[O_2]-diimine-dioximato site, as well a single chloride ion in the **Ni,M-Cl** cases or a κ^1-acetate group in the **Ni,M-OAc** cases. The geometry around M is *pseudo*-octahedral in each case, and the value of $\angle XMC_{cent}$ (the angle defined by the positions of the X atom (chloride or O of acetate), the metal center M (Rh or Ir), and the centroid of the η^5-Cp* ligand) spans a tight range of 126.3° to 133.2°. These values are similar to the values of corresponding angles measured in previously published crystallographic data for water-bound **Rh-OAc** and dimethylsulfoxide-bound **Ir-OAc** complexes averaging to 127.0° and 129.9°, respectively.[33,34] Considering the similarity of these values, we conclude that the acetate ligands in the [**Ni,M-OAc**] complexes do not interact strongly with the pendant nickel(II) site contained in the macrocyclic ligand.

The Ni•••M distances are slightly smaller for Rh (3.649(1) Å and 3.664(1) Å) versus Ir (3.677(1) Å and 3.725(1) Å), consistent with the larger ionic radius of Ir(III) (0.68 Å) vs. Rh(III) (0.66 Å).[35] This finding implies that Rh could serve as a stronger Lewis acid to modulate the properties of the nickel center in comparison to iridium. This is in agreement with the tabulated pK_a values of the corresponding aqua ions of Rh(III) and Ir(III), which show that Rh(III) is more Lewis acidic (pK_a = 3.4) than Ir(III) (pK_a = 4.4) in H_2O.[36] The average N–O bond distances in the bimetallic complexes of nickel range from 1.318(4) Å to 1.336(6) Å, either indistinguishable from or slightly smaller than the value of 1.336(3) Å found in the monometallic precursor **Ni**. This suggests modest π-bonding interactions occur from O to M, consistent with the electronic nature of Rh and Ir as 4*d* and 5*d* transition metals. Such π-bonding effects have been considered previously for the related bimetallic [Ni,Zn] complexes studied by Peters and co-workers.[20a]

Data from XRD analysis of the Co(III) complexes are generally similar to the data collected with the Ni(II) complexes. However, an interesting counterpoint in the data for the **Co-M-μ-OAc** complexes (Figure 3) is the observation of bridging acetate ligands that span the two different metal centers in the isomorphous structures. We were inspired to attempt installation of the bridging acetate ligands by the observation of such ligands in the work of Chaudhuri and co-workers.[19] Here, we anticipated that we could favor installation of bridging acetate ligands via generation of the synthon **Co-Cl**, which features a coordination site on Co(III) occupied in the monometallic precursor by presumably loosely bound CH_3CN; see Figure S10 in SI). On the basis of the observed structures, this bound CH_3CN could indeed be readily displaced by acetate associated with the incoming [Cp*M] fragment, generating the desired acetate bridges between Co(III) and M(III). Supporting this viewpoint, the structures of the **Ni,M-OAc** complexes lack these bridging acetates; this is attributable to the general preference of Ni(II) to retain its square-planar geometry in the heterobimetallic complexes.

As in the Ni(II) complexes, the Co(III) ion is situated in the tetradentate macrocyclic site in all cases. Indeed, the ω_{N4} values for the **Co-Cl$_2$** precursor as well as all the bimetallic cobalt complexes span a narrow range from 0.024–0.030, consistent with relative rigidity of the diimine-dioximato framework. On the other hand, inspection of the $\psi_{M'}$ values for the heterobimetallic complexes reveals a significant displacement of the Co(III) centers by 0.114–0.115 Å from the plane of the diimine-dioximato ligand. This displacement is readily attributable to coordination of the bridging acetate ligand, which appears to pull the cobalt ion out of the plane due to strain induced by two-point binding of the acetate ligand. Such a structural deformation of the M′ site may contribute to the electrochemical behavior of these complexes (*vide infra*).

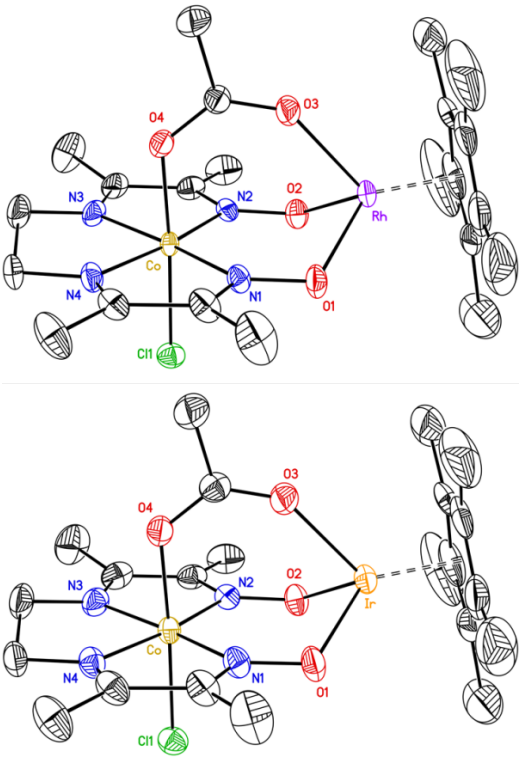

Figure 3. Solid-state structures from XRD of **Co,Rh-μ-OAc** (upper structure) and **Co,Ir-μ-OAc** (lower structure). All H-atoms and the outer-sphere hexafluorophosphate counteranion are omitted for clarity. Displacement ellipsoids are shown at the 50% probability level.

Surveying the complete family of structural results for the heterobimetallic complexes, a noticeable increase in the O1•••O2 interatomic distance (across the dioximato site) is apparent in comparisons to the corresponding values for the monometallic complexes **Ni** and **Co-Cl$_2$**. O1 and O2 play the crucial role of ligating M, and consistent with the large sizes of Rh and Ir, the O1•••O2 distance increases in all cases by 0.342-0.365 Å (see Table 1). This increased separation is attributable to the large size of the Rh and Ir centers in comparison to H^+ found in the monometallic complexes, although such comparisons are difficult to quantify directly. Considering the monometallic complexes alone, the O1•••O2 separation in **Co-Cl$_2$** is 0.28 Å greater than in **Ni** (2.697(1) vs. 2.420(2) Å, respectively), a situation attributable to the more sterically demanding propyl backbone present in **Ni**, which likely 'pushes' the macrocyclic oximato moieties together and assists in formation of a strong O–H•••O hydrogen bond. Consistent with this theory, the analogue of **Ni** prepared with an ethyl backbone has an O1•••O2 separation of 2.616(1) Å, significantly greater (nearly 0.2 Å) than the value for **Ni** with a propyl bridge.[20a] This is consistent with a pulling apart of the two 'sides' of the ligand away from the oxygens, and opening up of the H-bonded O1•••O2 site.

Within this family of analogous structures, there are noticeable trends in the Ni•••M and Co•••M distances. For the nickel complexes, the Ni•••M distances are very similar for the pairs containing the same metals; **Ni,Rh-Cl** and **Ni,Rh-OAc** have distances of 3.649(1) and 3.664(1) Å, respectively, while **Ni,Ir-Cl** and **Ni,Ir-OAc** have slightly longer distances of 3.677(1) and 3.725(1) Å, respectively. This high degree of similarity attests to the lack of strong interactions between the chloride and κ^1-acetate ligands bound to Rh/Ir with nickel, while the slightly larger values for the acetate complexes do indicate a role for steric bulk in 'opening' of the concave face of the heterobimetallic structures. Moreover, the slightly longer distances between Ni and Ir are consistent with the larger size of Ir in comparison to Rh. For the

pair of isomorphous cobalt complexes bridged by acetate ligands that interact with both metal centers, we note a significantly longer Co•••Ir distance of 3.643(1) Å versus a Co•••Rh distance of 3.606(1) Å. We anticipate that this and the 1.5° increase in the folding along the O1•••O2 vector are again attributable to the greater size of Ir in comparison to Rh and the fixed length of the acetate bridge. Finally, we note the M′•••M distances (where M′ is Ni or Co) are significantly larger for the nickel acetate complexes (3.664(1) and 3.725(1) Å, respectively) in comparison to the corresponding values for the cobalt acetate complexes (3.606(1) and 3.643(1) Å, respectively). These distances are consistent with the bridging role of the acetate ligand in the cobalt complexes, which draws the two metal centers together via two-point binding in the cobalt complexes.[37]

2.3 Electronic Absorption Spectroscopy

Dissolution of the isolated heterobimetallic complexes in CH_3CN results in orange to deep red solutions. To investigate the electronic properties of the compounds and compare them to the monometallic precursors, we turned to electronic absorption (EA) spectroscopy. The EA spectrum of **Co-Cl₂** displays a lowest energy absorption band in the near-UV region with a maximum absorption wavelength (λ_{max}) at 350 nm with a molar absorptivity (ε) of ca. 3600 M^{-1} cm^{-1} (Figure 4). Based on its intensity, we assign this feature as a charge transfer (CT) band. Upon replacement of the proton bridge with the [Cp*M] organometallic fragments in **Co,Rh-μ-OAc** and **Co,Ir-μ-OAc**, the compounds absorb more strongly in the visible region and display red-shifted lowest energy absorption bands (λ_{max} = 411 nm; ε = 4500 M^{-1} cm^{-1} and λ_{max} = 431 nm; ε = 4000 M^{-1} cm^{-1}, respectively) complexes (Figure 4). The shifts in the lowest energy absorption maxima to longer wavelengths suggest a particular influence of the second metal on the electronic properties of the heterobimetallic complexes. Similar behavior was observed by Peters & co-workers in a related nitrito-bridged bimetallic complex of the form [Co^{III}-μ-NO_2-Mg], which displayed a lowest energy absorption maximum at 418 nm.[20b] Considering the similarity of the results for this [Co,Mg] heterobimetallic complex to our own, we hypothesize that coordination of Lewis acidic metals to the dioximato ligand framework drives the shift in absorption to lower energies. Both of the heterobimetallic cobalt complexes studied here as well as **Co-Cl₂** exhibit additional bands at higher energies; these are attributable to intraligand π-to-π* transitions with molar absorptivity values greater than 20,000 M^{-1} cm^{-1} in all cases. Consistent with the distal placement of the Rh/Ir centers with respect to the conjugated ligand backbone around the Co(III) center, these higher energy bands are relatively unperturbed by coordination of the secondary metals.

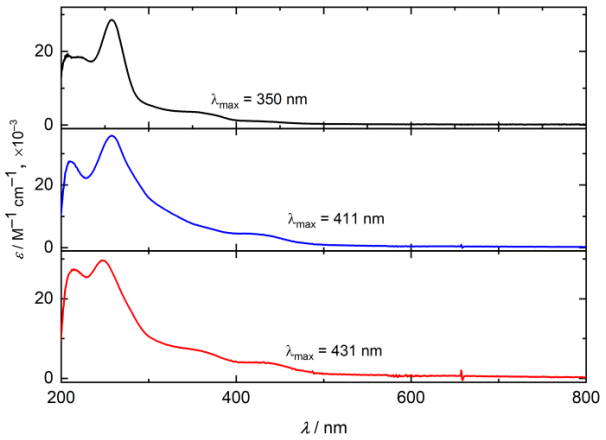

Figure 4. Stacked electronic absorption spectra for **Co-Cl₂** (black), **Co,Rh-μ-OAc** (blue) and **Co,Ir-μ-OAc** (red) in CH_3CN.

Similar to the heterobimetallic cobalt complexes, the heterobimetallic nickel complexes feature intraligand π-to-π* transitions in the UV region between 200 – 300 nm (ε > 15000 M^{-1} cm^{-1}) that strongly resemble bands present in the monometallic precursor **Ni** (see SI, Figure S28 for all spectra). Along with these intense features, the heterobimetallic complexes display intense CT bands around 400 nm in all cases. The CT bands are strikingly similar in their absorption maxima for the rhodium complexes **Ni,Rh-Cl** (λ_{max} = 397 nm; ε = 5200 M^{-1} cm^{-1}) and **Ni,Rh-OAc** (λ_{max} = 395 nm; ε = 10800 M^{-1} cm^{-1}) and also the iridium complexes **Ni,Ir-Cl** (λ_{max} = 385 nm; ε = 6700 M^{-1} cm^{-1}) and **Ni,Ir-OAc** (λ_{max} = 388 nm; ε = 9600 M^{-1} cm^{-1}). Notably, the λ_{max} values are slightly blue-shifted for the Ir complexes in comparison to the analogous Rh complexes, a finding that diverges from the results obtained with the cobalt complexes (*vide supra*). On the other hand, the acetate complexes have molar absorptivities that are much larger than for the analogous chloride complexes. Considered together with the ^{1}H NMR data (see SI), the electronic absorption spectra confirm that the heterobimetallic complexes are persistent in solution, resulting in the unique spectra obtained in each case. Thus, we next turned to electrochemical studies to understand how the multiple metals impact the redox properties of the heterobimetallic compounds.

2.4 Electrochemistry

A primary goal of our study is to understand the influence of the [Cp*Rh] and [Cp*Ir] moieties on the electrochemical properties of the redox-active Ni- or Co-containing diimine-dioximato cores. Since these cores are redox-active and frequently used in catalysis, we were particularly curious to see how the presence of heavy metals (Rh and Ir) might affect the redox properties of these metal-containing ligands. In order to understand any intrinsic reduction processes for Rh^{III} and Ir^{III} centers in our systems, however, we first performed control cyclic voltammetry (CV) experiments on the **M-OAc** precursors. In our studies, we observed single chemically irreversible cathodic waves at quite negative reduction potentials for both **Rh-OAc** ($E_{p,c}$ = –1.57 V vs $Fc^{+/0}$) and **Ir-OAc** ($E_{p,c}$ = –2.04 V vs $Fc^{+/0;}$ see SI, Figures S34 and S36). As the redox processes observed with the monometallic nickel and cobalt complexes as well as the heterobimetallics occur at significantly more positive potentials, we have tentatively considered the [Cp*M] fragments as redox-inactive at potentials positive of these potentials in the new compounds. However, bringing the Rh and Ir metal centers into proximity of the nickel and cobalt centers is not without consequence, as described below.

CV experiments have been previously performed on the parent monometallic complex **Ni** and the dibromide analogue of **Co-Cl₂** by Fontecave and co-workers.[14] Here, we re-confirmed the electrochemical properties of **Ni** and also collected fresh data for **Co-Cl₂** and **Co-Cl** (see SI, Figures S29, S31 and S33). The electrochemical data for **Ni** (see SI, Figure 29) revealed a chemically reversible reduction process at $E_{1/2}$ = –1.22 V vs the ferrocenium/ferrocene couple (denoted hereafter as $Fc^{+/0}$). This feature has been observed previously[14,20a] and has been assigned as a $Ni^{II/I}$ couple. Scan rate-dependent studies (see SI, Figure S30) revealed a linear dependence of both the cathodic and anodic peak currents on the square root of scan rate confirming freely diffusing nature of both isolated **Ni** as well as its reduced form. A second chemically reversible wave was also observed at a more negative potential ($E_{1/2}$ = –1.80 V vs $Fc^{+/0}$). Notably, this redox process was not mentioned in the prior work from Fontecave and co-workers, although a similar feature was measured by Peters and co-workers.[20] Based on the quite negative reduction potential, we anticipate that this feature may correspond to a ligand-centered reduction, but we did not pursue a rigorous assignment here.

Compared to the relatively clean voltammograms obtained with monometallic **Ni** (see SI, Figure S29), a more complex profile was obtained

when electrochemical studies were performed on the heterobimetallic complexes containing nickel. Qualitatively, voltammograms of all four isolated [Ni,M] complexes are similar and display a single, chemically irreversible cathodic wave near $E_{p,c}$ = –1.48 V vs $Fc^{+/0}$ (see SI, Figures S39–S42 for all the individual voltammograms). On the basis of the prior assignment of the first reduction of **Ni** as metal-centered from the work of Fontecave and co-workers, we assign this reduction as a Ni^{II}/Ni^{I} process. The reduced forms of the complexes are unstable, however, as judged by CV, as in all cases the voltammograms lack a coupled re-oxidation wave, confirming speciation of the complexes into one or more different forms upon reduction. Multiple irreversible reduction features occur when scanning to more negative potentials (see SI, Figures S39–S42), suggesting chemical speciation and the involvement of irreversible processes upon reduction of the [Ni,M] heterobimetallics. Considering the potentials involved, we anticipate that Rh- and/or Ir-centered reductions could be involved in this quite negative-potential redox chemistry. We have previously encountered chemically irreversible redox properties for half-sandwich rhodium complexes bearing select bidentate ligands, particularly in cases where the bidentate ligands are lost from the Rh metal center, promoting formation of dimeric and/or oligomeric complexes.[38] Considering the likely generation of an anionic Ni-containing fragment upon Ni-centered reduction, we anticipate such processes may be involved here.

On the other hand, the electrochemical properties of the heterobimetallic cobalt complexes displayed significantly more well-resolved electrochemical behavior. For comparison, the cyclic voltammogram of the monometallic **Co-Cl₂** complex (see Figure 5, black trace) displays a profile that can be assigned on the basis of prior work[14] as involving two separate $1e^-$ redox processes which are overlapping with each other; the more positive process can be assigned as $Co^{III/II}$ ($E_{1/2}$ = ca. –0.75 V) and the more negative to $Co^{II/I}$ ($E_{1/2}$ = –0.98 V vs $Fc^{+/0}$). Appealingly, all three accessible oxidation states of cobalt mentioned above are freely diffusing as judged by scan rate-dependent studies (see SI, Figure S32). The appearance of the CV data for the **Co-Cl₂** differs from that of the dibromide analogue measured by Fontecave and co-workers, in that the reduction potentials display a greater separation of 540 mV in comparison to the much more modest 220 mV or so measured here for **Co-Cl₂**. On the other hand, halide ligands are often lost upon reduction of Co^{III} to Co^{II}, a feature that could drive the small difference between the the $Co^{II/I}$ couple measured here for **Co-Cl₂** ($E_{1/2}$ = –0.98 V vs $Fc^{+/0}$) and that of the dibromide analogue ($E_{1/2}$ = –1.11 V vs $Fc^{+/0}$).[17] Furthermore, similar to the **Ni** case, the CV data of **Co-Cl₂** (see SI, Figure S31) display a further, even more negative reduction process at $E_{1/2}$ = –2.03 V vs $Fc^{+/0}$. Strikingly similar, although more complicated, features were generally observed in the electrochemical data of the monochloride species **Co-Cl** (see SI, Figure S33), possibly due to flexible coordination number of the Co center, leading to the presence of multiple species in solution that can undergo reduction.

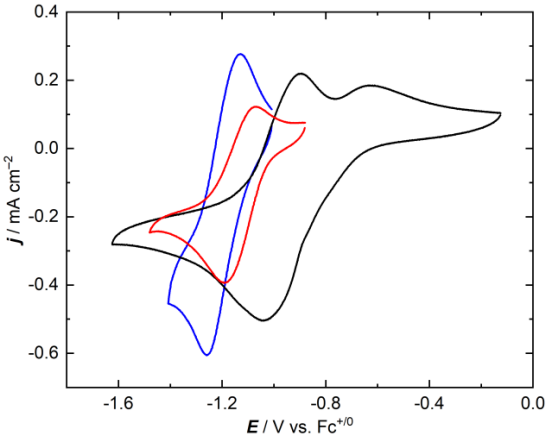

Figure 5. Cyclic voltammetry data for **Co-Cl₂** (black trace), **Co,Rh-μ-OAc** (blue trace) and **Co,Ir-μ-OAc** (red trace). Conditions: 0.1 M $[nBu_4N]^+[PF_6]^-$ in CH_3CN; scan rate: 100 mV/s; concentrations of all complexes were 2 mM.

To our delight, the CV profiles of the heterobimetallic complexes containing cobalt display a chemically reversible process at $E_{1/2}$ = –1.19 V vs $Fc^{+/0}$ for **Co,Rh-μ-OAc** and $E_{1/2}$ = –1.13 V vs $Fc^{+/0}$ for **Co,Ir-μ-OAc**. The voltammograms of both complexes display a return oxidation wave when the potential is switched after the first reduction process (Figure 5). We attribute this single electrochemically quasi-reversible and chemically reversible redox event to a $Co^{II/I}$ couple on the basis of its similarity to the $Co^{II/I}$ couple measured for **Co-Cl₂** as well as other cobalt complexes.[17] In addition, no further reductions were measured in the nearby potential range, suggesting shift of the corresponding $Co^{III/II}$ reduction to more positive potentials. However, similar to the [Ni,M] case, multiple irreversible reduction features occur in the cobalt heterobimetallic complexes when scanning more negative than –1.6 V or so (see SI, Figures S47 and S48), suggesting chemical speciation and instability of the reduced forms of the complexes at more negative potentials. Scan rate-dependent studies on the **Co,M-μ-OAc** (see SI, Figures S44 and S46) revealed a linear dependence of both the cathodic and anodic peak currents on the square root of scan rate confirming freely diffusing nature of Co^{II} and Co^{I} forms of the complexes.

Inspection of the $E_{1/2}$ values from the CV data of the [Co,M] complexes reveals that the values for the $Co^{II/I}$ reduction are shifted by ca. 150 – 200 mV) to more negative values in comparison to value for **Co-Cl₂** (Figure 5). This potential shift is attributable the substitution of the macrocyclic bridging proton with the Rh^{III} or Ir^{III} metal centers. These large metals engage in covalent bonding with the dioximato ligand framework and could afford inductive effects via π-interactions that give rise to the noted potential shifts. In accord with this theory, the average N–O distances of the oximato moieties in the bimetallic complexes are shorter by a modest 0.015 Å as compared to their values in the monometallic analogue. In this context, the effect of secondary metal coordination on the electrochemistry of nickel has been discussed previously by Peters & co-workers in reference to their [Ni,Zn] systems.[20a]

However, in comparison to the **Co,Ir-μ-OAc** complex, the $E_{1/2}$ value of the **Co,Rh-μ-OAc** complex is shifted 60 mV more negative. This shift is in opposition to the predicted trend on the basis of the Lewis acidity of Rh vs. Ir (*vide supra*) as well as the anticipated superior ability of Ir vs. Rh to engage in covalent bonding via more significant orbital overlap. However, these Lewis acidity and electronic arguments may be superceded by a structural effect, in that the Co•••M distances from the XRD data show that the Rh center is closer to Co by 0.037 Å as compared to the Ir center. This closeness, implying a possible tighter association of the acetate anion with cobalt in solution, would give rise

to the more negative $E_{1/2}$ value. Schelter and co-workers have observed similar discrepancies between Lewis acidity and structural effects in their notable work with heteromultimetallic complexes of redox-active cerium.[39]

Considering the noted shifts in redox chemistry and electronic properties, we carried out a preliminary investigation of possible influences of the assembled metals on a model catalytic reaction. For this preliminary investigation, we utilized the heterobimetallic [Co,Rh] complex in a test for catalysis of hydrogenation (see SI for details). For this study, we chose trifluoromethylbenzaldehyde (**A**) as a substrate, due to the general inertness of the aryl ring and trifluoromethyl group towards hydrogenation under our conditions and the ease of monitoring the reactions using ^{19}F NMR. The test was carried out at 50°C for 24 hours in CD_3CN with 1 atm of H_2 gas and a catalytic amount of triethylamine. With 7 mol% loading of **Co,Rh-μ-OAc**, an 80% conversion of **A** to its hydrogenated product, trifluoromethylbenzyl alcohol (**B**) was recorded (see SI, Figures S49 and S51). Notably, no conversion of **A** to **B** was observed when the hydrogenation experiment was performed in the presence of 10 mol% of the parent complex **Co-Cl₂** or in the absence of any metal complex (see SI, Figures S49 and S50). Low conversion (13%) was observed when 10 mol% of **Rh-OAc** was tested for catalysis (see SI, Figures S49 and S52). When the hydrogenation was performed with a 1:1 mixture of the individual monometallic precursor complexes (**Co-Cl₂** + **Rh-OAc**), significant conversion (40%) of **A** to **B** was observed, but concomitantly with observation of multiple other products, suggesting unselective reactivity (see SI, Figures S49 and S53). Thus, this preliminary study highlights an apparent advantage of [Co,Rh] toward hydrogenation, suggesting that our series of heterobimetallic complexes could be used in future studies of multimetallic chemistry.

3. DISCUSSION

This work shows that the dioximato moiety present in both **Ni** and **Co-Cl₂** is suitable for chelation of [Cp*Rh] and [Cp*Ir] species, building on the elegant prior work of Chaudhuri, Peters, and Cossairt.[19,20,21] Notably, Rh and Ir are heavier elements than the various metals previously installed into the dioximato-type sites, expanding the versatility of this ligand environment. All of this synthetic chemistry suggests, however, that the dioximato moiety is a relatively flexible coordination site, capable of stably holding both redox-inactive and redox-active metals at moderate distances from the primary metal of 3.6–3.7 Å.

The new heterobimetallic complexes described here are stable in solution, much like the macrocyclic [Ni,M] and [UO_2,M] complexes that we have studied in our prior work, but nonetheless lack macrocyclic stabilization.[11,12] On the other hand, the spectroscopic and electrochemical studies reveal only subtle influences of the secondary metals (Rh and Ir) on the properties of the first metal (Ni or Co). This situation of subtle tuning is attributable to the general similarity of Rh^{III} and Ir^{III}, however, considering their positions in the periodic table, sizes, and Lewis acidities.[36] In the current work, we anticipate that the small shifts in reduction potentials induced by the secondary metals can be concluded to be driven by structural factors promoted by the two-point acetate ligand binding and resultant electrostatic considerations.

Generally speaking, the utilization of *in situ* protonolysis reactivity with Cp*M(OAc)₂ to generate the new heterobimetallic complexes described here is reminiscent of other ligation reactions of [Cp*M] complexes.[40] For example, 2-phenylpyridine does not present intrinsically acidic C–H bonds but can readily undergo cyclometallation at Ir(III) upon inclusion of weak bases like acetate due to pre-coordination of the pyridine moiety that leads to acidification of an *ortho*-phenyl C–H bond. This reactivity resembles the *in situ* deprotonation of **Ni** and **Co-Cl₂** utilized here, leading to the clean and generally high-yielding synthesis of the new heterobimetallic complexes. Considering the presence of significant electron density on the O-atoms of the proton-bridged macrocyclic precursor complexes, we anticipate that the flexible coordination environment of the Cp*M(OAc)₂ and [Cp*MCl_2]₂ complexes could enable a similar pre-coordination of these complexes to an oxime oxygen, resulting in acidification of the macrocyclic bridging proton. Such a reaction sequence highlights the general utility of these synthons for generation of other heterobimetallic complexes on these platforms in the future, particularly via routes involving protonolysis reactivity of suitable precursors.

4. CONCLUSIONS

We have synthesized and characterized a family of heterobimetallic complexes by pairing diimine-monoxime-monooximato macrocyclic ligands containing nickel and cobalt centers and organometallic half-sandwich [Cp*M] (M = Rh, Ir) fragments with a protonolysis strategy. In the solid-state structures of the six new heterobimetallic complexes, the Ni(II) centers prefer square-planar geometry while the Co(III) centers favor octahedral geometry, promoting bridging interactions of acetate across Co and Rh/Ir. Installation of Rh or Ir in place of the bridging proton in the dioximato site results in significant changes in the electrochemical profiles in all cases, demonstrating the utility of the second metal in changing the properties of these complexes. Preliminary hydrogenation studies with **Co,Rh-μ-OAc** revealed clean catalytic conversion of a substituted benzaldehyde to benzyl alcohol and suggest a key role of the multiple metal sites in the reactivity. Taken together, these findings illustrate that heterobimetallic complexes of the type described here could find future applications in the exciting area of multimetallic chemistry and catalysis.

5. EXPERIMENTAL SECTION

5.1 General Considerations

All manipulations were carried out in dry N_2-filled gloveboxes (Vacuum Atmospheres Co., Hawthorne, CA) or under N_2 atmosphere using standard Schlenk techniques unless otherwise noted. All solvents were of commercial grade and dried over activated alumina using a PPT Glass Contour (Nashua, NH) solvent purification system prior to use, and were stored over molecular sieves. All chemicals were from major commercial suppliers and used as received or after extensive drying.

Ligands $(DOH)_2$en and $(DOH)_2$pn were prepared according to literature procedures.[27,28] [Cp*$RhCl_2$]₂ was synthesized according to the modified procedure reported by Sanford & co-workers, but the original procedure by Maitlis & co-workers was used in the synthesis of [Cp*$IrCl_2$]₂.[30] **M-OAc** complexes were synthesized using methods described by Medola.[41] **Ni** complex was prepared using a literature procedure described by Uhlig and Friedrich.[27] Spectroscopic characterizations of all of the above compounds by ^{1}H NMR (see SI, Figures S2 – S8) are in agreement with the prior literature reports.

Deuterated NMR solvents were purchased from Cambridge Isotope Laboratories (Tewksbury, MA, USA). ^{1}H, ^{31}P, and ^{19}F NMR spectra were collected on a 400 MHz Bruker spectrometer (Bruker, Billerica, MA, USA) and referenced to the residual protio-solvent signal[42] in the case of ^{1}H. ^{31}P and ^{19}F NMR spectra were referenced and reported relative to H_3PO_4 and CCl_3F, respectively, as external standards following the recommended scale based on ratios of absolute frequencies (Ξ).[43,44] Chemical shifts (δ) are reported in units of ppm and coupling constants (*J*) are reported in Hz. All experiments were conducted at room temperature (298 K). NMR spectra are given in the SI (Figures S2 to S28). Electronic absorption spectra were collected with an Ocean Optics Flame spectrometer equipped with DH-Mini light source, in a 1 cm path length quartz cuvette. Elemental analyses were performed by Midwest Microlab, Inc. (Indianapolis, IN, USA).

5.2 Electrochemical Methods

Electrochemical experiments were carried out in a N_2-filled glovebox in dry, degassed CH_3CN. 0.10 M tetra(*n*-butylammonium) hexafluorophosphate ($[^nBu_4N]^+[PF_6]^-$); Sigma-Aldrich, electrochemical grade) served as the solvent and supporting electrolyte. Measurements were carried out with a Gamry Reference 600+ Potentiostat/Galvanostat (Gamry Instruments, Warminster, PA, USA), using a standard three-electrode configuration. The working electrode was the basal plane of highly oriented pyrolytic graphite (HOPG) (GraphiteStore.com, Buffalo Grove, Ill.; surface area: 0.09 cm^2), the counter electrode was a platinum wire (Kurt J. Lesker, Jefferson Hills, PA; 99.99%, 0.5 mm diameter), and a silver wire immersed in electrolyte served as a pseudoreference electrode (CH Instruments). The reference was separated from the working solution by a Vycor frit (Bioanalytical Systems, Inc., West Lafayette, IN, USA). Ferrocene (Sigma Aldrich, St. Louis, MO, USA; twice-sublimed) was added to the electrolyte solution prior to the beginning of each experiment; the midpoint potential of the ferrocenium/ferrocene couple (denoted as $Fc^{+/0}$) served as an external standard for comparison of the recorded potentials. Concentrations of analytes for cyclic voltammetry were typically 2 mM unless otherwise noted. Experiments were conducted by first scanning cathodically, then anodically on the return sweep.

5.3 Synthesis and characterization of monometallic cobalt complexes and heterobimetallic complexes

Synthesis of **Co-Cl$_2$**. The monometallic Co complex was synthesized by modification of a literature procedure.[28] A solution of anhydrous $CoCl_2$ (86 mg, 0.66 mmol) in dry methanol was added dropwise to a methanolic solution of $(DOH)_2$en (150 mg, 0.66 mmol) in air. A dark red solution was obtained, which was stirred for 3-4 hours in air until the observation of brown-colored precipitate. The brown precipitate was filtered on a frit and washed with cold methanol. This procedure is slightly different from the reported synthesis, in that the authors filtered the dark red solution after 20 minutes of stirring and allowed the filtrate to evaporate slowly in air. Yield = 60% (140 mg). Spectroscopic characterization by ^{1}H NMR (see SI, Figure S9) confirmed preparation of the desired compound, formulated as $CoCl_2(DOH)(DO)$en. ^{1}H NMR (400 MHz, CD_3CN): δ 13.85 (bs, 1H, *H4*), 4.66 (s, 4H, *H3*), 2.55 (t, $^5J_{H\text{-}H}$ = 1.4 Hz, 6H, *H1*), 2.43 (s, 6H, *H2*) ppm.

Synthesis of **Co-Cl**. In an inert atmosphere glovebox and in the dark, a solution of $AgPF_6$ (110 mg, 0.42 mmol) in acetonitrile was added dropwise to a solution of **Co-Cl$_2$** (160 mg, 0.45 mmol) in acetonitrile. The mixture was stirred overnight, and the resulting AgCl precipitate was filtered on a frit. The filtrate was evaporated *in vacuo* to give a dark yellow solid. Yield = 94% (190 mg). Spectroscopic characterization by ^{1}H, ^{19}F, and ^{31}P NMR (see SI, Figures S10 – S12) confirmed isolation of the desired synthon, formulated as $[CoCl(NCCH_3)(DOH)(DO)en]PF_6$. ^{1}H NMR (400 MHz, CD_3CN): δ 9.77 (bs, 1H, *H4*), 4.68 (s, 4H, *H3*), 2.59 (s, 6H, *H1*), 2.46 (s, 6H, *H2*), 1.96 (s, 3H, *H5*) ppm. ^{19}F NMR (376 MHz, CD_3CN) δ –73.70 (d, $^1J_{F,P}$ = 706 Hz) ppm. ^{31}P NMR (162 MHz, CD_3CN) δ –145.48 (q, $^1J_{P,F}$ = 706 Hz) ppm

Synthesis of **Ni,M-Cl**. A solution of $NaOAc\cdot 3H_2O$ (70 mg, 0.50 mmol) in dichloromethane was added dropwise to a mixture of **Ni** (200 mg, 0.50 mmol) and $[Cp^*MCl_2]_2$ (**M** = **Rh**: 155 mg, 0.2; **M** = **Ir**: 200 mg, 0.25 mmol) in dichloromethane The mixture was stirred overnight, and the resulting NaCl precipitate was filtered over a celite plug. The filtrate was evaporated *in vacuo*. The resulting solid was washed with toluene multiple times to remove unreacted $[Cp^*MCl_2]_2$ and with $CHCl_3$ to remove unreacted **Ni**. The resultant reddish-brown solid in each case was dried to not more than 50°C to give the pure product. Vapor diffusion of Et_2O into a concentrated CH_3CN solution of **Ni,Rh-Cl** yielded single crystals suitable for X-ray diffraction studies. Vapor diffusion of Et_2O into a concentrated CH_3OH solution of **Ni,Ir-Cl** yielded single crystals suitable for X-ray diffraction studies. Spectroscopic characterizations by ^{1}H NMR (see SI, Figures S13 and S14) confirmed preparation of the desired compounds, formulated as $[Ni(DOH)(DO)pnCp^*RhCl]ClO_4$ and $[Ni(DOH)(DO)pnCp^*IrCl]ClO_4$, respectively. **Ni,Rh-Cl**: Yield = 88% (298 mg). ^{1}H NMR (400 MHz, CD_3CN) δ 3.26 – 3.17 (m, 2H, *H4*), 3.02 – 2.91 (m, 2H, *H4*), 2.09 (t, $^5J_{H\text{-}H}$ = 1.5 Hz, 6H, *H2*), 1.99 (s, 6H, *H3*), 1.64 (s, 15H, *H1*) ppm. Anal. Calcd for $C_{21}H_{33}Cl_2N_4NiO_6Rh$: C 37.65, H 4.96, N 8.36; Found: C 35.51, H 4.40, N 7.72. Calcd for $C_{21}H_{33}Cl_2N_4NiO_6Rh + CH_2Cl_2 + 0.5\ CH_3CN$: C 35.62, H 4.74, N 8.13. This analysis is consistent with the observation of tightly associated CH_2Cl_2 and CH_3CN in ^{1}H NMR (despite extensive drying) as well as consistent with the presence of co-crystallized CH_3CN in the XRD data for **Ni,Rh-Cl** (see the Supporting Information). **Ni,Ir-Cl**: Yield = 94% (360 mg). ^{1}H NMR (400 MHz, CD_3CN) δ 3.26 – 3.16 (m, 2H, *H4*), 3.06 – 2.96 (m, 2H, *H4*), 2.10 (t, $^5J_{H\text{-}H}$ = 1.5 Hz, 6H, *H2*), 1.97 (s, 6H, *H3*), 1.60 (s, 15H, *H1*) ppm. Anal. Calcd for $C_{21}H_{33}Cl_2N_4NiO_6Ir$: C 33.22, H 4.38, N 7.38; Found: C 33.50, H 4.23, N 7.36.

Syntheses of **Ni,M-OAc**. Under nitrogen, a solution of **M-OAc** (**M** = **Rh**: 150 mg, 0.42 mmol; **M** = **Ir**: 185 mg, 0.42 mmol) in dry dichloromethane was added dropwise to a solution of **Ni** (165 mg, 0.42 mmol) in dry dichloromethane. The dark red solution was stirred for 1-2 h, and the volatiles were evaporated *in vacuo* to give a reddish-brown solid in each case. The solid was washed with diethyl ether to remove leftover acetic acid and then dried to not more than 50°C to give the pure product. In both cases, vapor diffusion of Et_2O into a concentrated CH_3CN solution was employed to obtain single crystals suitable for X-ray diffraction. Spectroscopic characterizations by ^{1}H NMR (see SI, Figures S15 and S16) confirmed preparation of the desired compounds, formulated as $[Ni(DOH)(DO)pnCp^*Rh(OCOCH_3)]ClO_4$ and $[Ni(DOH)(DO)pnCp^*Ir(OCOCH_3)]ClO_4$, respectively. **Ni,Rh-OAc**: Yield = 94% (270 mg). ^{1}H NMR (400 MHz, CD_3CN) δ 3.57 (d, *J* = 15.8 Hz, 2H, *H4*), 3.13 (t, *J* = 13.7 Hz, 2H, *H4*), 2.30 (s, 3H, *H6*), 2.11 (s, 6H, *H2*), 2.00 (s, 6H, *H3*), 1.61 (s, 15H, *H1*) ppm. Anal. Calcd for $C_{23}H_{36}ClN_4NiO_8Rh$: C 39.83, H 5.23, N 8.08; Found: C 39.51, H 4.97, N 7.86. **Ni,Ir-OAc**: Yield = 91% (296 mg). ^{1}H NMR (400 MHz, CD_3CN) δ 3.29 – 3.21 (m, 2H, *H4*), 3.06 – 2.94 (m, 2H, *H4*), 2.39 (s, 3H, *H6*), 2.13 (s, 6H, *H2*), 2.00 (s, 6H, *H3*), 1.57 (s, 15H, *H1*) ppm. Anal. Calcd for $C_{23}H_{36}ClN_4NiO_8Ir$: C 35.28, H 4.63, N 7.16; Found: C 34.23, H 4.85, N 6.96. Calcd for $C_{23}H_{36}ClN_4NiO_8Ir + H_2O$: C 34.49, H 4.78, N 7.00. This analysis is consistent with the presence of tightly associated H_2O in the in the isolated compound, despite careful handling, and is consistent with consistent observation of H_2O in the isolated material by ^{1}H NMR (see the Supporting Information).

Syntheses of **Co,M-μ-OAc**. Under nitrogen, a solution of **M-OAc** (**M** = **Rh**: 160 mg, 0.45 mmol; **M** = **Ir**: 200 mg, 0.45 mmol) in dry dichloromethane was added dropwise to a solution of **Co-Cl** (190 mg, 0.41 mmol) in dry dichloromethane. The dark red solution was stirred for 1-2 h, and the volatiles were removed *in vacuo* to give a yellowish-brown solid in each case. On a bed of celite, the solid was washed with toluene to remove acetic acid and excess **M-OAc**. Washings with diethyl ether were given to remove toluene. The residue on the celite bed was then flushed with dichloromethane, and the filtrate evaporated to give a pure product which was then dried to not more than 50°C. In both cases, vapor diffusion of Et_2O into a concentrated CH_3CN solution was employed to obtain single crystals suitable for X-ray diffraction. Spectroscopic characterizations by ^{1}H NMR (see SI, Figures S17 – S22) confirmed preparation of the desired compounds, formulated as $[CoCl(DOH)(DO)pnCp^*Rh(\mu\text{-}OCOCH_3)]PF_6$ and $[CoCl(DOH)(DO)pnCp^*Ir(\mu\text{-}OCOCH_3)]PF_6$, respectively. **Co,Rh-μ-OAc**: Yield = 90% (280 mg). ^{1}H NMR (400 MHz, CD_3CN) δ 4.41

(m, 4H, *H4*), 2.50 (s, 3H, *H2*), 2.41 (s, 6H, *H3*), 1.68 (s, 6H, *H5*), 1.65 (s, 15H, *H1*) ppm. ^{19}F NMR (376 MHz, CD_3CN) δ −73.80 (d, $^1J_{F,P}$ = 706 Hz) ppm. ^{31}P NMR (162 MHz, CD_3CN) δ −145.50 (q, $^1J_{P,F}$ = 706 Hz) ppm. Anal. Calcd for $C_{22}H_{34}ClCoF_6N_4O_4PRh$: C 34.73, H 4.50, N 7.36; Found: C 35.10, H 4.53, N 7.21. [**Co,Ir-μ-OAc**]: Yield = 85% (295 mg). ^{1}H NMR (400 MHz, CD_3CN) δ 4.43 (m, 4H, *H4*), 2.47 (s, 3H, *H2*), 2.41 (s, 6H, *H3*), 1.70 (s, 6H, *H5*), 1.58 (s, 15H, *H1*) ppm. ^{19}F NMR (376 MHz, CD_3CN) δ −73.70 (d, $^1J_{F,P}$ = 708 Hz) ppm. ^{31}P NMR (162 MHz, CD_3CN) δ −145.49 (q, $^1J_{P,F}$ = 708 Hz) ppm. Anal. Calcd for $C_{22}H_{34}ClCoF_6N_4O_4PIr$: C 31.08, H 4.03, N 6.59; Found: C 29.31, H 3.65, N 5.76. Calcd for $C_{22}H_{34}ClCoF_6N_4O_4PIr + CH_2Cl_2$: C 29.54, H 3.88, N 5.99. This analysis is consistent with the observation of tightly associated CH_2Cl_2 in isolated samples of [**Co,Ir-μ-OAc**] by ^{1}H NMR (see the Supporting Information).

5.4 Synthesis and characterization of other monometallic complexes.

In the course of these studies, monometallic complexes of [Cp*M] bearing bidentate dimethylglyoxime and diphenylglyoxime ligands were also prepared and fully characterized. These complexes are [Cp*Ir(dmg)Cl]Cl, [Cp*Rh(dpg)Cl]PF_6, and [Cp*Ir(dpg)Cl]Cl where dmg is κ^2-dimethylglyoxime and dpg is κ^2-diphenylglyoxime. Notably, in the course of completing the work described here, Kuwata and co-workers reported the synthesis and characterization of [Cp*Ir(dmg)Cl]Cl.[45]

Synthesis of **dmgIr-Cl**. A solution of $[Cp^*IrCl_2]_2$ (100 mg, 0.12 mmol) in dichloromethane was added dropwise to a solution of dimethylglyoxime (29 mg, 0.25 mmol) in MeOH. The mixture was stirred for 12 h, and the volatiles were removed *in vacuo* to give an orange solid. Vapor diffusion of Et_2O into a concentrated CH_3OH solution of **dmgIr-Cl** was employed to obtain single crystals suitable for X-ray diffraction studies. Spectroscopic characterization by ^{1}H NMR (see SI, Figure S23) is in agreement with the prior literature report.[45] Yield = 90% (115 mg). ^{1}H NMR (400 MHz, CD_3OD) δ 2.41 (s, 6H, *H3*), 1.77 (s, 15H, *H1*) ppm. Anal. Calcd for $C_{14}H_{23}Cl_2N_2O_2Ir$: C 32.69, H 4.51, N 5.45; Found: C 32.53, H 4.11, N 5.37.

Synthesis of **dpgRh-Cl**. A solution of $[Cp^*RhCl_2]_2$ (180 mg, 0.29 mmol) in dichloromethane was added dropwise to a mixture of diphenylglyoxime (150 mg, 0.62 mmol) and $AgPF_6$ (158 mg, 0.62 mmol) in methanol. The mixture was stirred for 12 h, and the volatiles were removed *in vacuo* to give a yellow solid. Vapor diffusion of Et_2O into a concentrated CH_2Cl_2 solution of **dpgRh-Cl** was employed to obtain single crystals suitable for X-ray diffraction studies. Spectroscopic characterizations by ^{1}H, ^{19}F, and ^{31}P NMR (see SI, Figures S24 – S26) confirmed preparation of the desired compound, formulated as [Cp*Rh(dpg)Cl]PF_6. Yield = 90% (370 mg). ^{1}H NMR (400 MHz, CD_3OD): δ 7.34 – 7.21 (m, 6H, *H3*), 7.14 – 7.09 (m, 4H, *H3*), 1.82 (s, 15H, *H1*) ppm. ^{19}F NMR (376 MHz, CD_3OD) δ −75.34 (d, $^1J_{F,P}$ = 709 Hz) ppm. ^{31}P NMR (162 MHz, CD_3OD) δ −145.37 (q, $^1J_{P,F}$ = 709 Hz) ppm. Anal. Calcd for $C_{24}H_{27}ClF_6N_2O_2PRh$: C 43.76, H 4.13, N 4.25; Found: C 43.51, H 4.31, N 4.22.

Synthesis of **dpgIr-Cl**. A solution of $[Cp^*IrCl_2]_2$ (230 mg, 0.30 mmol) in dichloromethane was added dropwise to a solution of diphenylglyoxime (150 mg, 0.62 mmol) in methanol. The mixture was stirred for 24 h, and the volatiles were removed *in vacuo* to give a reddish-brown solid. Vapor diffusion of Et_2O into a concentrated CH_3CN solution of **dpgIr-Cl** was employed to obtain single crystals suitable for X-ray diffraction studies. Spectroscopic characterization by ^{1}H NMR (see SI, Figure S27) confirmed preparation of the desired compound, formulated as [Cp*Ir(dpg)Cl]Cl. Yield = 92% (365 mg). ^{1}H NMR (400 MHz, CD_3OD): δ 7.40 – 7.29 (m, 6H, *H3*), 7.19 – 7.12 (m, 4H, *H3*), 1.88 (s, 15H, *H1*) ppm. Anal. Calcd for $C_{24}H_{27}Cl_2N_3O_2Ir$: C 45.14, H 4.26, N 4.39; Found: C 45.30, H 4.42, N 3.86. Calcd for $C_{24}H_{27}Cl_2N_3O_2Ir + 0.6\ CH_3OH$: C 44.92, H 4.50, N 4.26. This analysis is consistent with association of CH_3OH with isolated **dpgIr-Cl**, consistent with observation of this solvent impurity by ^{1}H NMR (see the Supporting Information).

ASSOCIATED CONTENT

Supporting Information

Supporting Information is available free of charge on the ACS Publications website: Experimental details; synthesis and characterization of compounds used in this study; NMR spectra; crystallographic details; electronic absorption spectra; electrochemical data (PDF); Cartesian coordinates (XYZ) from single-crystal XRD studies.

Accesion Codes

CCDC entries 2079400–2079408 contain the supplementary crystallographic data for this paper. These data can be obtained free of charge via www.ccdc.cam.ac.uk/ data_request/cif, or by emailing data_request@ccdc.cam.ac. uk, or by contacting The Cambridge Crystallographic Data Centre, 12 Union Road, Cambridge CB2 1EZ, UK; fax: +44 1223 336033.

AUTHOR INFORMATION

Corresponding Author

* To whom correspondence should be addressed. E-mail: blakemore@ku.edu, phone: +1 (785) 864-3019 (J.D.B.)

Author Contributions

The manuscript was written through contributions of all authors. All authors have given approval to the final version of the manuscript.

Current Adresses

† Current address: Department of Chemistry, University of Chicago, 5735 S. Ellis Avenue, Chicago, Illinois 60637, United States

Note

The authors declare no competing financial interests.

ACKNOWLEDGMENT

The authors thank Dr. Justin Douglas and Sarah Neuenswander for assistance with NMR spectroscopy and Prof. Davide Lionetti for assistance with the preliminary refinement of solid-state XRD data. This work was supported by the US National Science Foundation through award OIA-1833087. Preliminary synthetic work was supported by the US National Science Foundation through the NSF REU Program in Chemistry at the University of Kansas (CHE-1560279). The authors also acknowledge the US National Institutes of Health for support of the NMR instrumentation used in this study (S10OD016360 and S10RR024664).

[1] Cooper, B. G.; Napoline, J. W.; Thomas, C. M. Catalytic Applications of Early/Late Heterobimetallic Complexes. *Catal. Rev.* **2012,** *54*, 1-40.

[2] Buchwalter, P.; Rosé, J.; Braunstein, P. Multimetallic catalysis based on heterometallic complexes and clusters. *Chem. Rev.* **2015**, *115*, 28–126.

[3] (a) McEvoy, J. P.; G. W. Brudvig, G. W. Water-splitting chemistry of photosystem II. *Chem. Rev.* **2006**, *106*, 4455–4483. (b) Yano, J.; Yachandra, V. Mn_4Ca Cluster in Photosynthesis: Where and How Water is Oxidized to Dioxygen. *Chem. Rev.* **2014**, *114*, 4175–4205.

[4] Tsukihara, T.; Shimokata, K.; Katayama, Y.; Shimada, H.; Muramoto, K.; Aoyoma, H.; Mochizuki, M.; Shinzawa-Itoh, K.; Yamashita, E.; Yao, M.; Ishimura, Y.; Yoshikawa, S. The low-spin heme of cytochrome *c* oxidase as the driving element of the proton-pumping process. *Proc. Natl. Acad. Sci. USA* **2003**, *100*, 15304.

[5] Spatzal, T.; Aksoyoglu, M.; Zhang, L. M.; Andrade, S. L. A.; Schleicher, E.; Weber, S.; Rees, D. C.; Einsle, O. Evidence for interstitial carbon in nitrogenase FeMo cofactor. *Science* **2011**, *334*, 940.

[6] (a) Volbeda, A.; Martin, L.; Cavazza, C.; Matho, M.; Faber, B. W.; Roseboom, W.; Albracht, S. P. J.; Garcin, E.; Rousset, M.; Fontecilla-Camps, J. C. Structural differences between the ready and unready oxidized states of [NiFe] hydrogenases. *J. Biol. Inorg. Chem.* **2005**, *10*, 239. (b) Bachmeier, A.; Armstrong, F. Solar-driven proton and carbon dioxide reduction to fuels - lessons from metalloenzymes. *Curr. Op. Chem. Biol.* **2015,** *25*, 141-151.

[7] Appel, A. M.; Bercaw, J. E.; Bocarsly, A. B.; Dobbek, H.; DuBois, D. L.; Dupuis, M.; Ferry, J. G.; Fujita, E.; Hille, R.; Kenis, P. J. A.; Kerfeld, C. A.; Morris, R. H.; Peden, C. H. F.; Portis, A. R.; Ragsdale, S. W.; Rauchfuss, T. B.; Reek, J. N. H.; Seefeldt, L. C.; Thauer, R. K.; Waldrop, G. L. Frontiers, opportunities, and challenges in biochemical and chemical catalysis of CO2 fixation. *Chem. Rev.* 2013, *113*, 6621.

[8] Tsui, E. Y.; Tran, R.; Yano, J.; Agapie, T. Redox-inactive metals modulate the reduction potential in heterometallic manganese-oxido clusters. *Nat. Chem.* **2013**, *5*, 293.

[9] Lee, Y.-M.; Bang, S.; Kim, Y. M.; Cho, J.; Hong, S.; Nomura, T.; Ogura, T.; Troeppner, O.; Ivanović-Burmazović, I.; Sarangi, R.; Fukuzumi, S.; Nam, W. A mononuclear nonheme iron(iii)–peroxo complex binding redox-inactive metal ions. *Chem. Sci.* **2013**, *4*, 3917.

[10] Li, F.; Van Heuvelen, K. M.; Meier, K. K.; Münck, E.; Que, L. Sc^{3+}-Triggered Oxoiron(IV) Formation from O_2 and its Non-Heme Iron(II) Precursor via a Sc^{3+}–Peroxo–Fe^{3+} Intermediate. *J. Am. Chem. Soc.* **2013**, *135*, 10198-10201.

[11] Kumar, A.; Lionetti, D.; Day, V. W.; Blakemore, J. D. Trivalent Lewis Acidic Cations Govern the Electronic Properties and Stability of Heterobimetallic Complexes of Nickel. *Chem. Eur. J.* **2018,** *24*, 141-149.

[12] Kumar, A.; Lionetti, D.; Day, V. W.; Blakemore, J. D. Redox-Inactive Metal Cations Modulate the Reduction Potential of the Uranyl Ion in Macrocyclic Complexes. *J. Am. Chem. Soc.* **2020,** *142*, 3032-3041.

[13] Kelsey, S.; Kumar, A.; Oliver, A. G.; Day, V. W.; Blakemore, J. D. Promotion and Tuning of the Electrochemical Reduction of Hetero- and Homobimetallic Zinc Complexes. *ChemRxiv* **2021**, Pre-Print, doi: 10.26434/chemrxiv.14230406.v1

[14] Jacques, P.-A.; Artero, V.; Pécaut, J.; Fontecave, M. Cobalt and nickel diimine-dioxime complexes as molecular electrocatalysts for hydrogen evolution with low overvoltages. *Proc. Natl. Acad. Sci. U.S.A* **2009,** *106*, 20627-20632.

[15] McCrory, C. C.; Uyeda, C.; Peters, J. C. Electrocatalytic hydrogen evolution in acidic water with molecular cobalt tetraazamacrocycles. *J. Am. Chem. Soc.* **2012,** *134*, 3164-3170.

[16] (a) Schrauzer, G. N. Organocobalt chemistry of vitamin B12 model compounds (cobaloximes). *Acc. Chem. Res.* **1968,** *1*, 97-103 (b) Connolly, P.; Espenson, J. H. Cobalt-catalyzed evolution of molecular hydrogen. *Inorg. Chem.* **1986,** *25*, 2684-2688 (c) Dempsey, J. L.; Winkler, J. R.; Gray, H. B. Mechanism of H_2 Evolution from a Photogenerated Hydridocobaloxime. *J. Am. Chem. Soc.* **2010,** *132*, 16774-16776.

[17] Laga, S. M.; Blakemore, J. D.; Henling, L. M.; Brunschwig, B. S.; Gray, H. B. Catalysis of Proton Reduction by a $[BO_4]$-Bridged Dicobalt Glyoxime. *Inorg. Chem.* **2014,** *53*, 12668-12670.

[18] Lance, K. A.; Goldsby, K. A.; Busch, D. H. Effective new cobalt(II) dioxygen carriers derived from dimethylglyoxime by the replacement of the linking protons with difluoroboron(1+). *Inorg. Chem.* **1990,** *29*, 4537-4544.

[19] Birkelbach, F.; Winter, M.; Floerke, U.; Haupt, H.-J.; Butzlaff, C.; Lengen, M.; Bill, E.; Trautwein, A. X.; Wieghardt, K.; Chaudhuri, P., Exchange Coupling in Homo-and Heterodinuclear Complexes CuIIM [M= Cr (III), Mn (III), Mn (II), Fe (III), Co (III), Co (II), Ni (II), Cu (II), Zn (II)]. Synthesis, Structures, and Spectroscopic Properties. *Inorganic Chemistry* **1994,** *33*, 3990-4001.

[20] (a) Uyeda, C.; Peters, J. C. Access to formally Ni (I) states in a heterobimetallic NiZn system. *Chem. Sci.* **2013,** *4*, 157-163. (b) Uyeda, C.; Peters, J. C. Selective nitrite reduction at heterobimetallic CoMg complexes. *J. Am. Chem. Soc.* **2013,** *135*, 12023-12031.

[21] Henckel, D. A.; Lin, Y. F.; McCormick, T. M.; Kaminsky, W.; Cossairt, B. M. A doubly deprotonated diimine dioximate metalloligand as a synthon for multimetallic complex assembly. *Dalton Trans.* **2016,** *45*, 10068-10075.

[22] Maitlis, P. M. (Pentamethylcyclopentadienyl)rhodium and -iridium complexes: approaches to new types of homogeneous catalysts. *Acc. Chem. Res.* **1978,** *11*, 301-307.

[23] (a) Brintzinger, H.; Bercaw, J. E. Bis(pentamethylcyclopentadienyl)titanium(II). Isolation and reactions with hydrogen, nitrogen, and carbon monoxide. *J. Am. Chem. Soc.* **1971,** *93*, 2045-2046. (b) Manriquez, J. M.; Bercaw, J. E. Preparation of a dinitrogen complex of bis(pentamethylcyclopentadienyl)zirconium(II). Isolation and protonation leading to stoichiometric reduction of dinitrogen to hydrazine. *J. Am. Chem. Soc.* **1974**, *96*, 6229-6230.

[24] (a) Kölle, U.; Grätzel, M. Organometallic Rhodium(III) Complexes as Catalysts for the Photoreduction of Protons to Hydrogen on Colloidal TiO_2. *Angew. Chem. Int. Ed. Engl.* **1987,** *26*, 567-570. (b) Blakemore, J. D.; Schley, N. D.; Balcells, D.;

Hull, J. F.; Olack, G. W.; Incarvito, C. D.; Eisenstein, O.; Brudvig, G. W.; Crabtree, R. H. Half-Sandwich Iridium Complexes for Homogeneous Water-Oxidation Catalysis. *J. Am. Chem. Soc.* **2010,** *132*, 16017-16029.

[25] (a) Boyd, E. A.; Lionetti, D.; Henke, W. C.; Day, V. W.; Blakemore, J. D. Preparation, Characterization, and Electrochemical Activation of a Model [Cp*Rh] Hydride. *Inorg. Chem.* **2019**, *58*, 3606-3615. (b) Hopkins, J. A.; Lionetti, D.; Day, V. W.; Blakemore, J. D. Chemical and Electrochemical Properties of [Cp*Rh] Complexes Supported by a Hybrid Phosphine-Imine Ligand. *Organometallics* **2019,** *38*, 1300-1310. (c) Hopkins, J. A.; Lionetti, D.; Day, V. W.; Blakemore, J. D. Synthesis and reactivity studies of a [Cp*Rh] complex supported by a methylene-bridged hybrid phosphine-imine ligand. *J. Organomet. Chem.* **2020**, *921*, 121294.

[26] Groom, C. R.; Bruno, I. J.; Lightfoot, M. P.; Ward, S. C. The Cambridge Structural Database. *Acta Cryst. B.* **2016,** *72*, 171-179.

[27] Uhlig, E.; Friedrich, M. Untersuchungen an Oximkomplexen. III. Nickelchelate des Bis-(diacetylmonoxim-imino)-propans-1,3 und des Bis-(diacetylmonoxim-imino)-äthans-1,2. *Z. Anorg. Allg. Chem.* **1966**, *343*, 299-307.

[28] Roy, A. S.; Weyhermüller, T.; Ghosh, P. A new cobalodioxime and its three levels of H-bondings to 1D helical strand, 2D helices and 3D framework. *Inorg. Chem. Commun.* **2008**, *11*, 167-170.

[29] Seeber, R.; Parker Jr, W. O.; Marzilli, P. A.; Marzilli, L. G. Electrochemical synthesis of Costa-type cobalt complexes. *Organometallics* **1989,** *8*, 2377-2381.

[30] (a) White, C.; Yates, A.; Maitlis, P. M.; Heinekey, D. M., (η^5-Pentamethylcyclopentadienyl)Rhodium and -Iridium Compounds. *Inorg. Synth.* **1992**, *29*, 228-234. (b) Mantell, M. A.; Kampf, J. W.; Sanford, M. Improved Synthesis of $[Cp^RRhCl_2]_2$ Complexes. *Organometallics* **2018,** *37*, 3240-3242.

[31] Jacques, P.-A.; Artero, V.; Pecaut, J.; Fontecave, M. CCDC 738487: Experimental Crystal Structure Determination, **2010**, DOI: 10.5517/ccssg55

[32] Roy, A.S.; Weyhermuller, T.; Ghosh, P. CCDC 646793: Experimental Crystal Structure Determination, **2008**, DOI: 10.5517/ccpq19q

[33] Jardim, G. A. M.; da Silva Júnior, E. N.; Bower, J. F. Overcoming naphthoquinone deactivation: rhodium-catalyzed C-5 selective C–H iodination as a gateway to functionalized derivatives. *Chem. Sci.* **2016,** *7*, 3780-3784.

[34] Frasco, D. A.; Lilly, C. P.; Boyle, P. D.; Ison, E. A. Cp^*Ir^{III}-Catalyzed Oxidative Coupling of Benzoic Acids with Alkynes. *ACS Catal.* **2013,** *3*, 2421-2429.

[35] Shannon, R. D. Revised effective ionic radii and systematic studies of interatomic distances in halides and chalcogenides. *Acta Cryst. A* **1976**, *32*, 751-767.

[36] D. D. Perrin, *Ionisation Constants of Inorganic Acids and Bases in Aqueous Solution*, Pergamon Press, New York, **1982**.

[37] (a) D'Souza, F.; Zandler, M. E.; Deviprasad, G. R.; Kutner, W. Acid-Base Properties of Fulleropyrrolidines: Experimental and Theoretical Investigations. *J. Phys. Chem. A* **2000,** *104*, 6887-6893. (b) D'Souza, F.; Chitta, R.; Gadde, S.; Zandler, M. E.; Sandanayaka, A. S. D.; Araki, Y.; Ito, O. Supramolecular porphyrin-fullerene via 'two-point' binding strategy: axial-coordination and cation-crown ether complexation. *Chem Commun.* **2005**, *10*, 1279-1281.

[38] (a) Lionetti, D.; Day, V. W.; Lassalle-Kaiser, B.; Blakemore, J. D. Multiple binding modes of an unconjugated bis(pyridine) ligand stabilize low-valent [Cp*Rh] complexes. *Chem. Commun.* **2018,** *54*, 1694-1697. (b) Lionetti, D.; Day, V. W.; Blakemore, J. D. Structural and chemical properties of half-sandwich rhodium complexes supported by the bis(2-pyridyl)methane ligand. *Dalton Trans.* **2019,** *48*, 12396-12406.

[39] Robinson, J. R.; Gordon, Z.; Booth, C. H.; Carroll, P. J.; Walsh, P. J.; Schelter, E. J., Tuning Reactivity and Electronic Properties through Ligand Reorganization within a Cerium Heterobimetallic Framework. *J. Am. Chem. Soc.* **2013**, *135*, 19016-19024.

[40] (a) Hu, Y.; Li, L.; Shaw, A. P.; Norton, J. R.; Sattler, W.; Rong, Y. Synthesis, Electrochemistry, and Reactivity of New Iridium(III) and Rhodium(III) Hydrides. *Organometallics* **2012,** *31*, 5058-5064. (b) Hull, J. F.; Balcells, D.; Blakemore, J. D.; Incarvito, C. D.; Eisenstein, O.; Brudvig, G. W.; Crabtree, R. H. Highly Active and Robust Cp* Iridium Complexes for Catalytic Water Oxidation. *J. Am. Chem. Soc.* **2009,** *131*, 8730-8731. (c) Davies, D. L.; Al-Duaij, O.; Fawcett, J.; Giardiello, M.; Hilton, S. T.; Russell, D. R. Room-temperature cyclometallation of amines, imines and oxazolines with $[MCl_2Cp^*]_2$ (M = Rh, Ir) and $[RuCl_2(p\text{-cymene})]_2$. *Dalton Trans.* **2003**, *21*, 4132-4138. (d) Scheeren, C.; Maasarani, F.; Hijazi, A.; Djukic, J.-P.; Pfeffer, M.; Zarić, S. D.; Le Goff, X.-F.; Ricard, L. Stereoselective "Electrophilic" Cyclometalation of Planar-Prochiral (η^6-Arene)tricarbonylchromium Complexes with Asymmetric Metal Centers: pseudo-T-4 $[Cp^*RhCl_2]_2$ and $[Cp^*IrCl_2]_2$. *Organometallics* **2007,** *26*, 3336-3345. (e) Hull, J. F.; Balcells, D.; Blakemore, J. D.; Incarvito, C. D.; Eisenstein, O.; Brudvig, G. W.; Crabtree, R. H. Highly Active and Robust Cp* Iridium Complexes for Catalytic Water Oxidation. *J. Am. Chem. Soc.* **2009**, *131*, 8730-8731.

[41] Boyer, P. M.; Roy, C. P.; Bielski, J. M.; Merola, J. S. Pentamethylcyclopentadienylrhodium bis-carboxylates: monohapto carboxylate coordination, dihapto carboxylate coordination, and water coordination to Cp∗Rh. *Inorg. Chim. Acta* **1996,** *245*, 7-15.

[42] Fulmer, G. R.; Miller, A. J. M.; Sherden, N. H.; Gottlieb, H. E.; Nudelman, A.; Stoltz, B. M.; Bercaw, J. E.; Goldberg, K. I. NMR Chemical Shifts of Trace Impurities: Common Laboratory Solvents, Organics, and Gases in Deuterated Solvents Relevant to the Organometallic Chemist. *Organometallics* **2010**, *29*, 2176-2179.

[43] Harris, R.K.; Becker, E.D.; Cabral de Menezes, S.M.; Goodfellow, R.; Granger, P. NMR nomenclature. Nuclear spin properties and conventions for chemical shifts (IUPAC Recommendations 2001). *Pure Appl. Chem.* **2001**, *73*, 1795-1818.

[44] Harris, R.K.; Becker, E.D.; Cabral de Menezes, S.M.; Granger, P.; Hoffman, R.E.; Zilm, K.W. Further conventions for NMR shielding and chemical shifts (IUPAC Recommendations 2008). *Pure Appl. Chem.* **2008**, *80*, 59-84.

[45] Takamura, T.; Harada, T.; Furuta, T.; Ikariya, T.; Kuwata, S. Half-Sandwich Iridium Complexes Bearing a Diprotic Glyoxime Ligand: Structural Diversity Induced by Reversible Deprotonation. *Chem. Asian J.* **2020,** *15*, 72-78.

For Table of Contents Only:

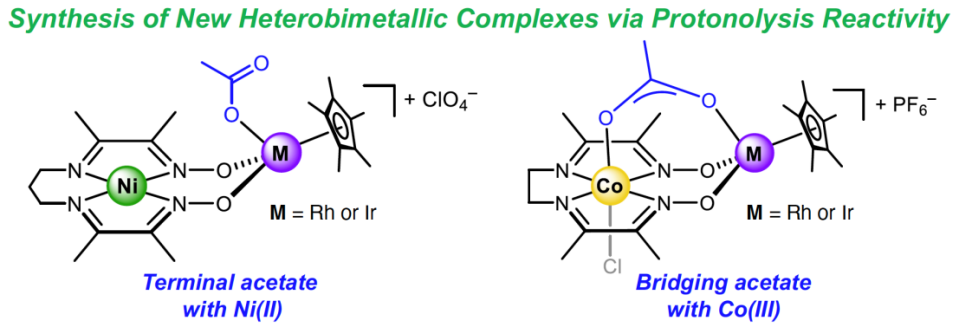

TOC Synopsis: A family of new heterobimetallic complexes incorporating half-sandwich rhodium and iridium species has been synthesized and fully characterized. Protonolysis reactivity was used to install the rhodium and iridium centers in the dioximato sites of macrocyclic nickel and cobalt complexes. Spectroscopic, electrochemical, and preliminary catalytic studies confirm the stability of the heterobimetallic complexes in solution and suggest these platforms may be useful in future studies of heterobimetallic chemistry and catalysis.